This is a repository copy of *An interactive visualization and data portal tool (PALTIDE) for relative sea level and palaeotidal simulations of the northwest European shelf seas since the Last Glacial Maximum*.

White Rose Research Online URL for this paper:
https://eprints.whiterose.ac.uk/210820/

Version: Published Version

Article:

An interactive visualization and data portal tool (PALTIDE) for relative sea level and palaeotidal simulations of the northwest European shelf seas since the Last Glacial Maximum

JAMES SCOURSE,[1]* SOPHIE WARD,[2] ADAM WAINWRIGHT,[2] SARAH BRADLEY,[3] JEROME KEATON WILSON[4] and JESSICA GUO[4]

[1]Department of Earth and Environmental Sciences, University of Exeter, Penryn Campus, Penryn, Cornwall, UK
[2]Marine Centre Wales, School of Ocean Sciences, Bangor University, Menai Bridge, Anglesey, UK
[3]Department of Geography, University of Sheffield, Sheffield, UK
[4]Arizona Experiment Station, University of Arizona, Tucson, AZ, USA

ABSTRACT: Relative sea level (RSL) predictions based on glacial isostatic adjustment (GIA) simulations and palaeotidal predictions generated by hydrodynamic models using GIA-generated palaeotopographies are available in the published literature, and datasets are available via data repositories. However, these data are often difficult to extract for specific locations or timeslices, requiring users to request datasets from corresponding authors. To overcome the intractability of these data and to enable users to interrogate datasets themselves without requiring offline requests, we have developed PALTIDE, an online visualization tool with intuitive user interface accessible at https://shiny.bangor.ac.uk/paleotidal/. The model domain for this interactive visualization tool is the northwest European continental shelf, covering the period from the Last Glacial Maximum (LGM) to the present day, and is based on previous GIA simulations by Bradley and colleagues and hydrodynamic simulations using Regional Ocean Modelling System (ROMS) published by Ward and colleagues. The tool is developed in R and utilizes a number of packages including *shiny* and *bslib* for the frontend, and *arrow*, *raster* and the *tidyverse* for backend data processing. The tool enables visualizations and data downloads for RSL, tidal amplitude and tide-dependent parameters for any location within the model domain over 1000-year timesteps from the LGM to the present.
© 2024 The Authors. *Journal of Quaternary Science* Published by John Wiley & Sons Ltd.

KEYWORDS: Holocene; Last Glacial Maximum; northwest Europe; palaeotidal; sea level

Introduction

Since the Last Glacial Maximum (LGM; 26.5–19 ka; Clark et al., 2009), the changes in the surface distribution of the oceans, ice sheets and land – driven by changes in orbitally modulated insolation and carbon cycle feedbacks – have fundamentally influenced all components of the Earth system. Ice sheets control the position of coastlines through both glacio-eustasy and glacio-isostasy and, in so doing, modulate ocean circulation and dynamics. The combined influences of glacio-eustasy and glacio-isostasy on palaeotopographic evolution and relative sea level (RSL) through both space and time can be simulated using glacial isostatic adjustment (GIA) models (Lambeck, 1995, 1996; Peltier, 1994; Bradley et al., 2023). GIA models integrate the time-dependent controls (e.g. deformation of the solid Earth) of RSL with input data from numerical ice sheet and solid Earth models and observations (Shennan et al., 2006; Bradley et al., 2023). Sea-level index points (SLIPs) provide the fundamental observational data by which GIA simulations are constrained (Bradley et al., 2023), and an iterative approach is usually adopted to improve the goodness-of-fit between the GIA simulations and the SLIP observations of RSL change. GIA simulations have become fundamental tools in Quaternary science over the past few

decades. The integrative nature of GIA modelling means that GIA simulations are now central to both the sea-level and palaeoglaciological research communities, providing a structured and reasoned basis for defining hypotheses for field/observational testing (Scourse, 2013).

Since they provide simulations of coastline and bathymetric change, palaeotopographies generated by GIA simulations are, in turn, fundamental inputs for 'palaeotidal' models. Palaeotidal simulations of shelf sea and coastal tidal amplitude are reconstructed using hydrodynamic models (e.g. POM, POLCOMS, OTIS, ROMS) that incorporate the major tidal forcings with input from global tidal models, with a boundary usually set at the shelf break. Early palaeotidal model simulations used a fixed topography with sea level defined by only eustatic change (e.g. Austin, 1991). Later palaeotidal modelling efforts included GIA simulations, which provide dynamic palaeotopography (i.e. includes RSL changes) and which more closely approximates geological observational data used to constrain palaeotidal model simulations (Scourse et al., 2002; Uehara et al., 2006; Scourse, 2013). Sensitivity tests using palaeotidal model simulations that integrate GIA topography for northwest Europe (Uehara et al., 2006; Ward et al., 2016) indicate that the response of the shelf tides during deglaciation are more sensitive to the ocean tide input than they are to inputs derived from different generations of GIA model inputs. Global tidal model inputs have improved

*Correspondence: James Scourse, as above.
Email: j.scourse@exeter.ac.uk

significantly in recent years, particularly for the period since the LGM through the subsequent period of deglaciation and the Holocene (e.g. Egbert et al., 2004; Green, 2010; Wilmes and Green, 2014; Schmittner et al., 2015; Wang et al., 2020; Lee et al., 2022; Sulzbach et al., 2023) with ongoing advances in computational and modelling capacity. The output from these global palaeotidal models provide key inputs to regional simulations by supplying tidal conditions at model boundaries, such as palaeotidal elevation amplitude and tidal current conditions.

Palaeotidal model simulations have become a powerful tool in Earth systems science since they hindcast the evolution of tidal amplitudes and tide-dependent parameters (bed stress, shelf sea stratification, tidal currents, dissipation of tidal energy) as coastlines and bathymetry change in response to RSL. Palaeotidal model simulations have a number of predictive/hindcasting applications. Simulated palaeotidal amplitudes are important for constraining SLIPs (Shennan et al., 2000; Neill et al., 2010; Ward et al., 2016), which rely on accurate assessment of vertical reference datums, such as mean high water spring tide; palaeotidal amplitudes (18–16 ka BP) from Ward et al. (2016) were used to constrain SLIPs within isolation basins in southwest Norway, in the construction of a revised RSL of the region (Vasskog et al., 2019). In turn, SLIPs are integral to GIA models of vertical crustal motion. Reconstructions of the spatial distribution and timing of seasonal stratification (and the associated tidal mixing fronts) in shelf sea environments are important for understanding fluxes of organic material to the seabed and hence for constraining the evolution of the role of shelf sea environments in the global carbon cycle (e.g. Rippeth et al., 2008; Scourse, 2013). For example, reconstructions of the timing of seasonal stratification in the western Irish Sea (Ward et al., 2016) were compared by Woods et al. (2019) with an age–depth model for a data point within the region, and the authors highlighted the importance of data points for validating and/or constraining palaeotidal model output. Assessments of the dissipation of tidal energy in the global ocean have implications for deep ocean circulation (Green et al., 2009; Wilmes and Green, 2014; Wilmes et al., 2021). Palaeotidal simulations of changes in the extent of the inter-tidal zone have archaeological implications (Mortimer et al., 2013; Barnett et al., 2020). Tidal current and bed shear stress predictions from palaeotidal simulations provide a means of hindcasting shelf sea sediment dynamics (e.g. van der Molen and de Swart, 2001; Scourse et al., 2009; Van Landeghem et al., 2009), with some of the inherent limitations and challenges discussed in Ward et al. (2020). Such large-scale distribution of shelf sea sediments by hydrodynamic processes has implications for coastal and geological basin evolution, and for understanding the contribution that shelf seas play in blue carbon sediment dynamics/habitats and carbon burial on continental shelves; it is this application that is the focus of the Convex Seascape Survey (https://convexseascapesurvey.com).

We have developed an open access online interactive visualization tool (PALTIDE) that enables users to interrogate and download RSL and palaeotidal simulation output via a user-friendly portal. Hitherto these data have been restricted to the palaeotidal community(ies) responsible for developing the simulations and therefore have been inaccessible unless through direct request. The tool enables users to visualize and download data for any location within the model domain in 1000-year timesteps from the LGM (taken here as 21 ka BP) to the present. These data can then be cited in any subsequent publication or outlet with reference to this paper which provides the technical details underpinning the tool. The tool can be accessed at: https://shiny.bangor.ac.uk/paleotidal/.

Methods

PALTIDE online visualization tool: development, source code and data

The PALTIDE tool (https://shiny.bangor.ac.uk/paleotidal/) takes output from regional GIA and palaeotidal models and presents these data in a series of online visualizations. The tool is designed to be a straightforward, user-friendly dashboard that allows users to explore palaeotidal simulations via custom data visualizations and provide access to specific subsets of simulation data based on user-specified inputs. All datasets visualized through the web app (RSL and palaeotidal model output) were in XYZ data format (further details below). The tool is developed in R (R Core Team, 2023), and utilizes a number of packages including *shiny* (Chang et al., 2023) and *bslib* (Sievert et al., 2023) for the frontend, and *arrow* (Richardson et al., 2023), *raster* (Hijmans and van Etten, 2012) and the *tidyverse* (Wickham et al., 2019) for backend data processing. The archived source code associated with the initial release associated with this paper can be found at https://doi.org/10.5281/zenodo.10020155 and the full data shown in simulations can be found at https://doi.org/10.5281/zenodo.10020210. The app is designed to work on most modern web-browsers and has layout optimization for mobile devices.

Relative sea level dataset

The RSL data made available through PALTIDE are from the GIA model of Bradley et al. (2011). This GIA model (specifically constrained for the British Isles) incorporates an ice sheet model developed by Bassett et al. (2005) with constraints on regional ice distribution by Shennan et al. (2006) and Brooks et al. (2008); full descriptions of the GIA model inputs and set-up are described in these source papers. The Bradley et al. (2011) GIA model integrates an ice model that underestimates British–Irish Ice Sheet ice volume and extent, as published by the BRITICE-CHRONO Project (http://www.britice-chrono.group.shef.ac.uk; Clark et al., 2022). Work is ongoing to incorporate revised GIA simulations, based on the BRITICE-CHRONO data on ice sheet thickness, extent and timings (Bradley et al., 2023), into new palaeotidal model simulations; this will result in an updated version of the online visualization tool (hereafter referred to as the 'tool') in due course. The palaeotopographies of the palaeotidal model (the latter is described below) combine the modern shelf bathymetry with these changes in RSL output by the Bradley et al. (2011) GIA model.

Hydrodynamic model set-up

The hydrodynamic model used is the three-dimensional Regional Ocean Modelling System (ROMS) (Shchepetkin and Mc Williams, 2005) as applied and described by Ward et al. (2016). The model iteration applied generates simulations based on the M_2 principal lunar semi-diurnal constituent, plus S_2 and N_2 constituents. The model has been used to generate simulations for 1000-year timesteps from the LGM, defined here as 21 ka BP, to the present; the timescales used are based on calibrated radiocarbon ages and so approximate the calendrical timescale. Output from a global ocean tidal model based on the Princeton Ocean Model (POM, Uehara et al., 2006) is used to force the shelf tides at the model boundaries. The palaeobathymetries used in the global model were prepared as described in Uehara et al. (2006) and integrate the global GIA simulations based on the ICE-5G (VM2) model (Peltier, 2004).

In the tool, individual datasets are all presented on the same ocean model grid, at ~1/24 degree spatial resolution (~2–3-km grid spacing). This resulted in 625 grid points from 15°W to 11°E, and 861 grid points in latitude from 45°N to 65°N (note that ROMS grids have varying spatial resolution with latitude). For consistency, the RSL datasets of Bradley et al. (2011) which were used within the palaeotidal modelling and which are visualized within this web application were linearly interpolated to the same ocean model grid.

Palaeotidal model output

The ROMS model outputs user-specified variables within a NetCDF file. Here, we use model outputs of tidal elevation amplitudes, depth-averaged (two-dimensional) tidal current speeds and near-bed tidal induced bed shear stress, and simulated tidal current speeds and model water depth are used in the calculation of seasonal stratification. Further details on how these model variables are computed are given below. The relevant variables were extracted from the raw NetCDF model output files and were saved as separate ASCII files, in XYZ data format, with each entry representing a variable value at a model grid point. Each visualization layer (velocity, bed shear stress, etc.) has its own set of ASCII files, with one datafile for each timeslice, 0–21 ka BP.

Simulated bed shear stress

Shelf sea sediment transport is driven by frictional forces exerted on the seabed, referred to as bed shear stress (τ_0, Equation 1). These bed shear stresses can be exerted by tides, waves, or combined tide plus wave motion, and are expressed as the force exerted by the flow per unit area of bed in terms of the density of water (ρ) and the frictional velocity (u_*) such that:

$$\tau_0 = \rho u_*^2 \tag{1}$$

Sediment transport (of non-cohesive sediments) occurs when the bed shear stress exceeds the threshold of motion. Changes in the current regime, such as through changes in sea level, thus directly impact on seabed sediment transport. Simulations of bed shear stress changes over time can help us understand the evolution of large-scale sediment patterns and features. For example, in some areas with large sand banks such as in the East China Sea (e.g. Uehara et al., 2002) and in the Celtic Sea (e.g. Belderson et al., 1986; Scourse et al., 2009), modern hydrodynamic conditions do not appear to be sufficiently energetic for their generation, indicating that they are a product of past current regimes. As such, the three-dimensional hydrodynamic model presented here was set to output 'near-bed' bed-shear stress (BSS), computed at the mid-depth of the bottom computational cell (as opposed to being calculated from depth-averaged tidal current speeds). The equations for computing the eastwards (τ_x, Equation 2) and northwards (τ_y, Equation 3) components of BSS are:

$$\tau_x = C_D(\sqrt{u^2 + v^2})u \tag{2}$$

$$\tau_y = C_D(\sqrt{u^2 + v^2})v \tag{3}$$

where τ is the BSS, C_D is the user-defined drag coefficient, and u and v are the simulated tidal current velocities in the east and north directions, respectively. The quadratic bottom drag scheme implemented, using a bottom drag coefficient of 0.003, was in line with other ROMS modelling studies of the region (e.g. Hashemi and Neill, 2014; Lewis et al., 2015; Robins et al., 2015). Note that no morphodynamic bed level changes (e.g. erosion, sedimentation) are implemented in the simulations as a feedback response to simulated bed shear stresses.

Calculation of seasonal stratification

Tidal mixing fronts are an important feature of many shelf seas that delineate seasonally stratified and well-mixed (or sporadically stratified) waters. This seasonal stratification is a key driver in biological, ecological and biogeochemical characteristics of shelf sea waters, and plays a key role in mediating the primary productivity of a region. Vertical stratification of the water column is driven by heating of surface waters, and where the vertical mixing of the water column is strong enough (predominantly by tidal stirring), this vertical stratification cannot occur. Tidal mixing fronts reside within the zone where the input of kinetic energy from the tides balances the heat input from solar radiation (Simpson and Hunter, 1974). As such, the positions of shelf sea tidal mixing fronts vary both seasonally and with the spring–neap tidal cycle.

Seasonally stratified continental shelf seas can act as net sinks for atmospheric carbon dioxide (CO_2). The flooding of the northwest European shelf seas during the last deglacial increased the areal extents of seasonally stratified continental shelf waters. This increase in seasonally stratified waters will in turn have contributed to increased drawdown of atmospheric CO_2 (during the summer months) on the modern northwest European shelf seas relative to the early deglacial period (Rippeth et al., 2008).

Much of the northwest European shelf seas are characterized by strong tidal currents, which are closely linked to seasonal stratification. Simpson and Hunter (1974) determined that the approximate location of the tidal mixing front in the Irish Sea is dependent upon water depth and tidal current speed. Bowers and Simpson (1987) then inferred that the locations of the tidal mixing fronts (on European seas) are consistent with a critical contour (or 'stratification parameter') at $\chi = 250$ m^{-2} s^{-3}, using the simulated depth-averaged M$_2$ tidal current speed (u, Equation 4). It is common to use the $\log_{10}$ value, and thus the equation becomes:

$$\chi = \log 10\left(\frac{h}{|u^3|}\right) \tag{4}$$

where h is water depth. It is this $\log_{10}$ value of the stratification parameter which is used here to approximate the position of the tidal mixing front, with a critical contour plotted at $\chi = 2.4$ (Bowers and Simpson, 1987). Areas characterized by $\chi < 1.9$ can be expected to remain well-mixed throughout the year, whereas vertically stratified waters can be expected where $\chi > 2.9$. So-called 'transition zones' are characterized by $1.9 < \chi < 2.9$, where this represents modulation in the position of the tidal mixing front within this zone due to seasonal heating and the spring–neap cycle.

PALTIDE: description

The online visualization tool, PALTIDE, is constructed around two pages

1. The landing page, which includes brief information on the tool, funder information and contact details, and explains how users are to cite downloaded data.
2. The data visualizations page, which allows the user to explore, visualize and download the full suite of palaeotidal model output and RSL datasets upon which the app is based.

The landing page is self-explanatory; here, we explain the main functions of the data visualizations page (Figure 1) and provide additional metadata on each of the downloadable datasets.

Data visualizations

From the landing page, the user can access the full functionality by clicking on the 'Explore Data Visualisations' tab. On this second page, within the 'Maps' section the user may visualize two-dimensional colour (raster) plots (hereafter referred to as 'maps', for ease) of various datasets (Figure 2), as well as download point-location data (Figures 3 and 4). Once on this page, the user must first select an ocean model output to view, with the options being:

1. Tidal amplitude: tidal elevation amplitude of the M_2 tidal constituent.
2. Stratification: with categorical data for mixed/frontal/stratified.
3. Peak Bed Stress: simulated magnitude and direction of near-bed peak tide-induced bed shear stress, output directly from the model, i.e. based on M_2, S_2 and N_2 tidal constituents (in $N\,m^{-2}$).
4. Tidal Current: simulated peak current speed of the M_2 tidal constituent, as an absolute magnitude (in $m\,s^{-1}$).

The user may then select whether to interrogate the maps (which is the default option) or whether to view a pre-generated animation of the loaded variable, by switching between the 'Interactive' or 'Animated' tabs [Figure 1, label (ii)]. An animation is available for each of the four variables listed above, and illustrates the maps one at a time, at 1000-year time-steps, from 21 ka BP forwards in time to the present (0 ka BP). The user may view the different animations by changing the variable within the drop-down menu called 'Data Selection'. There is a slight delay when moving between different model parameters, or when changing the period being visualized. All efforts were taken to minimize this delay, but we have prioritized high-resolution data over run speed.

The user may zoom in on the raster map by using either the +/− sign at the top left of the map panel, or by using the scrolling function on a mouse (scroll wheel). To move the map, simply click and drag the image. For each map, light grey colours indicate land (the ocean model 'land mask'), whereas white areas illustrate the 'ice mask' within the ocean model (the latter visible from 9 ka BP and earlier, Figure 1). For peak bed stress, the colour map illustrates the absolute magnitude of the bed stress ($N\,m^{-2}$) and the white vector arrows show the associated direction of peak bed stress. For app run speed, it was necessary to downscale and filter the full suite of bed shear stress vectors in the map to show only those vectors representing bed shear stress $>0.5\,N\,m^{-2}$ and spatially downscaled to only plot every 100 of those (note this does not affect downloaded data).

Additional user-defined options

To the top right of the visualization page is a slider, where the user can choose the time period/year to be visualized in the colour-plot (in 1-ka timeslices). The period to view can be changed by clicking and dragging the slider, or by clicking on discrete points on the scale. Below the timeline is a checkbox option for including the modern coastline ('show modern coastline') on the maps (black line). The contemporary coastline is a shapefile from NOAA's global coastline (Wessel and Smith, 1996) and the 'low-resolution' coastline is used here for app runtime.

Timeseries plots of RSL and tidal amplitude

The user may click on any point within the raster map [Figure 1, label (iii)], using the cursor (a hand), which brings up a 'pin' at the selected location. For any user-defined point location the corresponding time-dependent RSL and tidal elevation amplitude data will be illustrated in the double y-axis line graph to the bottom right of the visualization page (Figure 3), with the title of the plot corresponding to the coordinates of that point location. The x-axis on the line graph is time, from 21 to 0 ka BP. No tidal amplitude points are
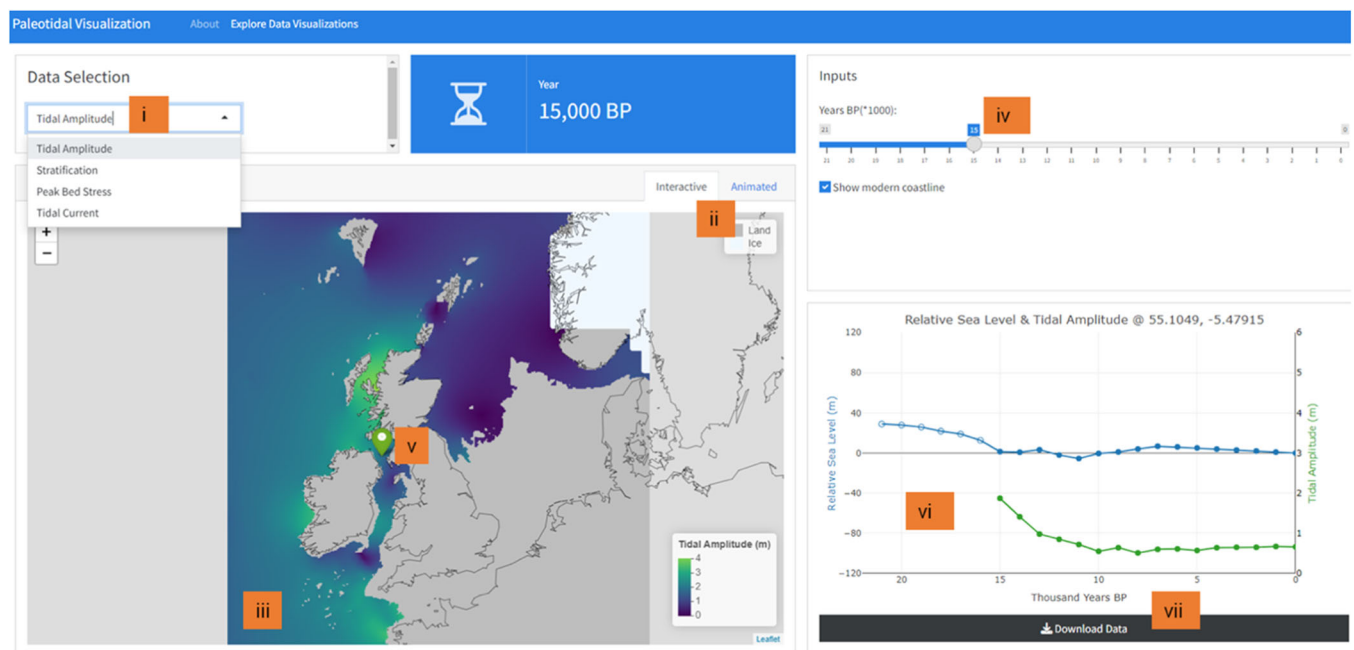

Figure 1. Data visualizations page showing (i) choice of model variable to view and (ii) an option to explore the interactive map or load an animation of the selected variable. While on the interactive maps (iii), further user-defined options include (iv) simulation timeslice to load and view. By clicking on the map and selecting a point location (v) the timeseries data for RSL and tidal elevation amplitude are plotted for that location (vi). Using the data download button (vii) the user may download the data associated with the variable loaded in the map. [Color figure can be viewed at wileyonlinelibrary.com]
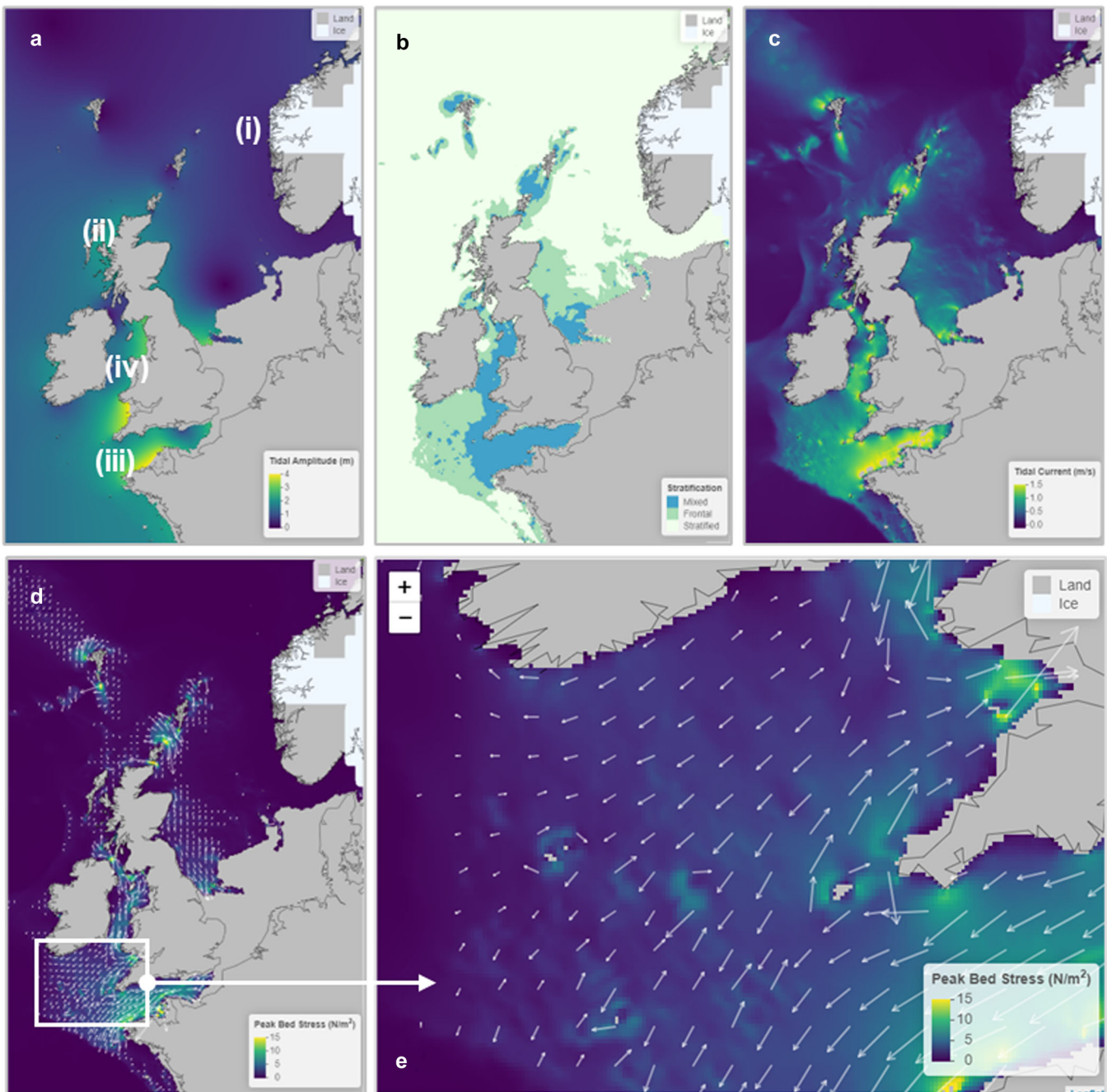
Figure 2. Example two-dimensional raster plots (maps) of (a) tidal elevation amplitude, (b) seasonal stratification, (c) tidal current speeds, and (d) bed shear stress speed (colour-scale) and direction (white vector arrows). (e) A zoomed-in illustration of the bed shear stress vectors, for the area indicated by the white bounding box in (d). All maps are for 10 ka BP. Labels (i)–(iv) on (a) are the approximate locations of the point data plotted in Figure 3. [Color figure can be viewed at wileyonlinelibrary.com]

plotted for timeslices when a point is not sea (referred to as 'water' throughout the app) within the ocean model (i.e. is land/under ice) and, as such, some datasets appear truncated in these plots. Note that no point data are available to visualize or download (described below) for points which have remined dry (i.e. land and/or ice) throughout all simulation timesteps. The user can hover the mouse over the datapoints and further quantitative information pops up (e.g. amplitude/rsl + year + landtype). The so-called 'landtype', i.e. whether a point is water/land/ice at each timeslice, is provided within the downloaded data (described in more detail below).

Data download

The data for a point location may be downloaded using the dark grey 'Download Data' button to the bottom right of the Data Visualisation page [Figure 1, label (vii)]. The data which are downloaded (Figure 4) are determined by the variable (model output) loaded in the map [label (a) in Figure 1]. Data available to download for point locations are:

1. Relative sea level (in metres below contemporary level, where present-day RSL = 0).
2. Stratification.
3. Bed shear stress (u- and v-components as well as absolute magnitude, in N m^{-2}).
4. Tidal current (simulated peak current speed of the M_2 tidal constituent, as an absolute magnitude, in m s^{-1}).

The default file download names are self-explanatory but can easily be overwritten: Tidal Amplitude.csv, Stratification.csv, Peak Bed Stress.csv and Tidal Current.csv. The format of each.csv data table is latitude*longitude*variable for each 22-ka timeslice.
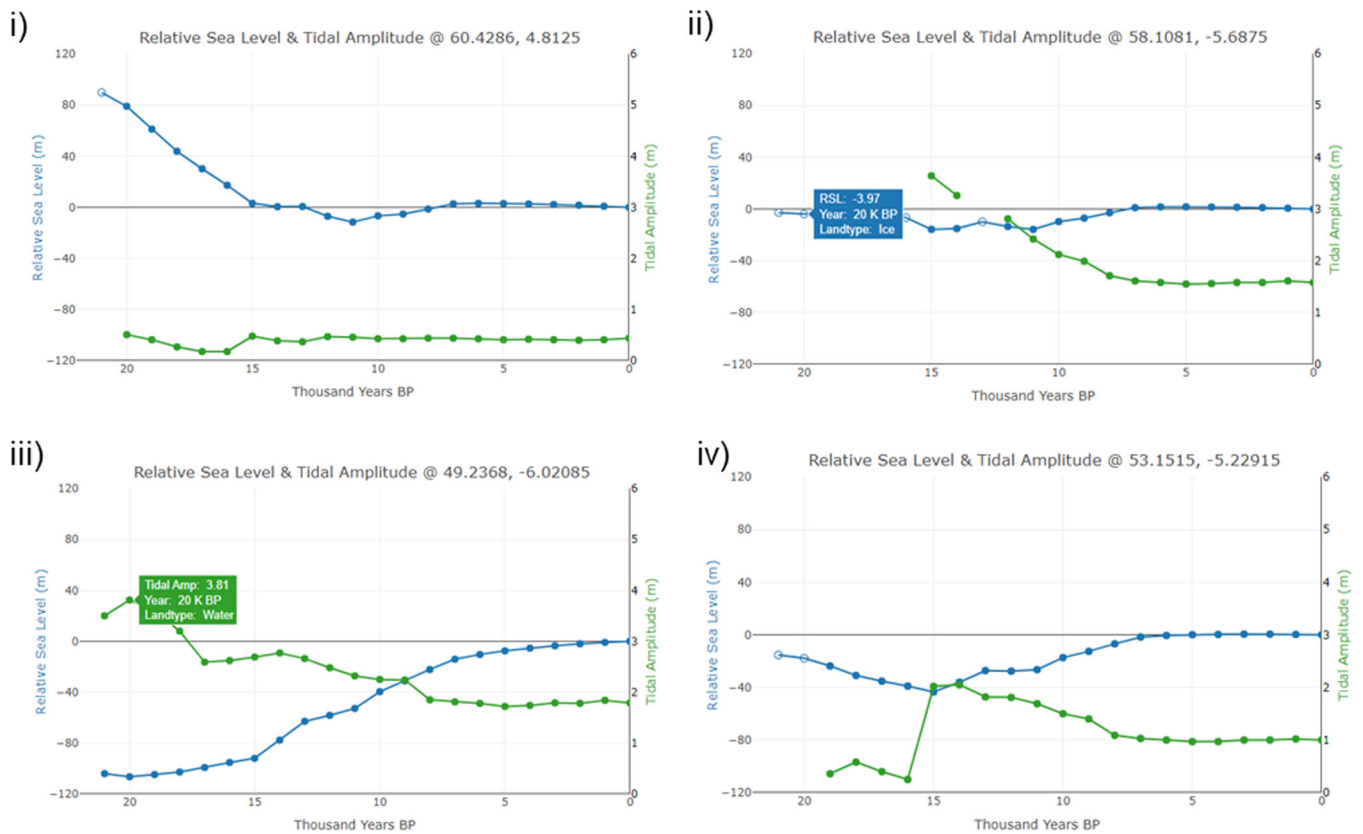
© 2024 The Authors. *Journal of Quaternary Science* Published by John Wiley & Sons Ltd.

Figure 3. Example plots of changes in RSL (left *y*-axes, blue lines) and tidal elevation amplitudes (right *y*-axes, green lines) with time (*x*-axes). The approximate point locations (i–iv) for which these data are plotted are given in Figure 2(a). [Color figure can be viewed at wileyonlinelibrary.com]

a

	A	B	C	D	E	F
1	longitude	latitude	year	land_type	rsl	elevation_amplitude
2	-4.9375	52.3951	0	water	0	1.2
3	-4.9375	52.3951	1	water	-0.02	1.21
4	-4.9375	52.3951	2	water	-0.16	1.14
5	-4.9375	52.3951	3	water	-0.58	1.12
6	-4.9375	52.3951	4	water	-1.21	1.07
7	-4.9375	52.3951	5	water	-1.92	1.06
8	-4.9375	52.3951	6	water	-3.14	1.12
9	-4.9375	52.3951	7	water	-5.03	1.21
10	-4.9375	52.3951	8	water	-11.03	1.4
11	-4.9375	52.3951	9	water	-17.72	1.9
12	-4.9375	52.3951	10	water	-23.7	2.04
13	-4.9375	52.3951	11	water	-34.26	2.21
14	-4.9375	52.3951	12	water	-36.94	2.28
15	-4.9375	52.3951	13	water	-38.48	2.41
16	-4.9375	52.3951	14	water	-49.41	2.45
17	-4.9375	52.3951	15	land	-59.51	NA
18	-4.9375	52.3951	16	land	-58.04	NA
19	-4.9375	52.3951	17	land	-57.02	NA
20	-4.9375	52.3951	18	land	-55.4	NA
21	-4.9375	52.3951	19	water	-51.74	0.34
22	-4.9375	52.3951	20	ice	-48.95	NA
23	-4.9375	52.3951	21	ice	-46.26	NA
24						

b

	A	B	C	D	E	F	G	H	I
1	longitude	latitude	year	rsl	elevation_amplitude	BSS_u	BSS_v	BSS_magnitude	land_type
2	-7.4375	48.02485	0	0	1.32	-0.85	-1.03	1.33	water
3	-7.4375	48.02485	1	-1	1.37	-0.88	-1.07	1.39	water
4	-7.4375	48.02485	2	-2.24	1.32	-0.84	-1.02	1.32	water
5	-7.4375	48.02485	3	-3.91	1.34	-0.85	-1.02	1.32	water
6	-7.4375	48.02485	4	-5.94	1.3	0.76	1.07	1.31	water
7	-7.4375	48.02485	5	-8.22	1.27	0.77	1.12	1.35	water
8	-7.4375	48.02485	6	-11.29	1.34	0.82	1.21	1.47	water
9	-7.4375	48.02485	7	-15.2	1.36	0.84	1.29	1.53	water
10	-7.4375	48.02485	8	-23.51	1.39	-1.14	-1.34	1.76	water
11	-7.4375	48.02485	9	-32.63	1.77	1.53	2.06	2.57	water
12	-7.4375	48.02485	10	-41.26	1.8	1.6	2.31	2.82	water
13	-7.4375	48.02485	11	-54.69	1.87	1.95	2.45	3.13	water
14	-7.4375	48.02485	12	-60.25	2.01	2.31	2.7	3.55	water
15	-7.4375	48.02485	13	-65.19	2.17	2.89	2.83	4.04	water
16	-7.4375	48.02485	14	-80.18	2.31	3.61	3.23	4.85	water
17	-7.4375	48.02485	15	-94.62	2.38	4.19	3.44	5.42	water
18	-7.4375	48.02485	16	-98.12	2.44	3.9	3.64	5.34	water
19	-7.4375	48.02485	17	-102.24	2.41	3.95	3.37	5.19	water
20	-7.4375	48.02485	18	-106.06	2.49	5.09	3.55	6.21	water
21	-7.4375	48.02485	19	-108.47	2.53	5.61	4.07	6.93	water
22	-7.4375	48.02485	20	-110.66	2.54	5.57	4.68	7.27	water
23	-7.4375	48.02485	21	-108.6	2.52	5.53	4.06	6.86	water
24									

Figure 4. Format of downloaded data for (a) tidal amplitude and (b) bed shear stress. In each, where ocean model outputs are not available (NA), the land_type column indicates whether the point was land or under ice at that timeslice. The tidal elevation amplitude and RSL are provided in all downloaded files.

Summary

The PALTIDE tool enables users to interrogate, download and visualize RSL and palaeotidal data for any location on the northwest European continental shelf for the period since the LGM based on the GIA simulations of Bradley et al. (2011) and the palaeotidal simulations of Ward et al. (2016). Because the data include site- and time-specific simulations of RSL as well as palaeotidal simulations of tidal amplitude, seasonal stratification, peak bed stress vectors and surface tidal currents, we anticipate that this tool will be of interest and value to a very wide range of user disciplines comprising Quaternary and marine geology, geophysics, Earth system science, sedimentology, marine ecology/biology, carbon cycle biogeochemistry, geomorphology, palaeo-climatology, palaeoceanography, sedimentology and archaeology. Later editions of the tool will include revised simulations for the northwest European continental shelf region based on GIA simulations integrating the BRITICE-CHRONO project ice sheet

observations (Bradley et al., 2023) and extension of the tool to all the global continental shelves using updated global GIA simulations. This work is ongoing funded by the Convex Seascape Survey (https://convexseascapesurvey.com/). Any data deriving from this first version of PALTIDE should cite this paper alongside Bradley et al. (2011) and Ward et al. (2016).

Data availability statement

The data that support the findings of this study are openly available in the app described in the paper.

Abbreviations. BSS, bed shear stress; GIA, glacial isostatic adjustment; LGM, Last Glacial Maximum; NOAA, National Oceanic and Atmospheric Administration; OTIS, One-Dimensional Transport with Inflow and Storage; POM, Princeton Ocean Model; POLCOMS, Proudman Oceanographic Laboratory Coastal Ocean Modelling System; RSL, relative sea level; ROMS, Regional Ocean Modelling System; SLIP, sea-level index point.

References

Austin, R.M. (1991) Modelling Holocene tides on the NW European continental shelf. *Terra Nova*, 3, 276–288.

Barnett, R.L., Charman, D.J., Johns, C., Ward, S.L., Bevan, A., Bradley, S.L. et al. (2020) Nonlinear landscape and cultural response to sea-level rise. *Science Advances*, 6, eabb6376.

Bassett, S.E., Milne, G.A., Mitrovica, J.X. & Clark, P.U. (2005) Ice sheet and solid earth influences on far-field sea-level histories. *Science*, 309, 925–928.

Belderson, R.H., Pingree, R.D. & Griffiths, D.K. (1986) Low sea-level tidal origin of Celtic Sea sand banks – evidence from numerical modelling of M2 tidal streams. *Marine Geology*, 73, 99–108.

Bowers, D.G. & Simpson, J.H. (1987) Mean position of tidal fronts in European-shelf seas. *Continental Shelf Research*, 7, 35–44.

Bradley, S.L., Ely, J.C., Clark, C.D., Edwards, R.J. & Shennan, I. (2023) Reconstruction of the palaeo-sea level of Britain and Ireland arising from empirical constraints of ice extent: implications for regional sea level forecasts and North American ice sheet volume. *Journal of Quaternary Science*, 38, 791–805.

Bradley, S.L., Milne, G.A., Shennan, I. & Edwards, R. (2011) An improved glacial isostatic adjustment model for the British Isles. *Journal of Quaternary Science*, 26, 541–552.

Brooks, A.J., Bradley, S.L., Edwards, R.J., Milne, G.A., Horton, B. & Shennan, I. (2008) Postglacial relative sea-level observations from Ireland and their role in glacial rebound modelling. *Journal of Quaternary Science*, 23, 175–192.

Chang, W., Cheng, J., Allaire, J., Sievert, C., Schloerke, B., Xie, Y. et al. (2023) shiny: web Application Framework for R. https://shiny.posit.co/.; https://github.com/rstudio/shiny

Clark, C.D., Ely, J.C., Hindmarsh, R.C.A., Bradley, S., Igneczi, A., Fabel, D. et al. (2022) Growth and retreat of the last British-Irish Ice Sheet, 31 000 to 15 000 years ago: the BRITICE-CHRONO reconstruction. *Boreas*, 51, 699–758.

Clark, P.U., Dyke, A.S., Shakun, J.D., Carlson, A.E., Clark, J., Wohlfarth, B. et al. (2009) The last glacial maximum. *Science*, 325, 710–714.

Egbert, G.D., Ray, R.D. & Bills, B.G. (2004) Numerical modeling of the global semidiurnal tide in the present day and in the last glacial maximum. *Journal of Geophysical Research: Oceans*, 109, C03003.

Green, J.A.M. (2010) Ocean tides and resonance. *Ocean Dynamics*, 60, 1243–1253.

Green, J.A.M., Green, C.L., Bigg, G.R., Rippeth, T.P., Scourse, J.D. & Uehara, K. (2009) Tidal mixing and the meridional overturning circulation from the Last Glacial Maximum. *Geophysical Research Letters*, 36, L15603.

Hashemi, M.R. & Neill, S.P. (2014) The role of tides in shelf-scale simulations of the wave energy resource. *Renewable Energy*, 69, 300–310.

Hijmans, R.J. & van Etten, J. (2012) raster: geographic analysis and modeling with raster data. R package version 2.0-12. http://CRAN.R-project.org/package=raster

Lambeck, K. (1995) Late devensian and Holocene shorelines of the British Isles and North Sea from models of glacio-hydro-isostatic rebound. *Journal of the Geological Society*, 152, 437–448.

Lambeck, K. (1996) Glaciation and sea-level change for Ireland and the Irish Sea since late devensian/midlandian time. *Journal of the Geological Society*, 153, 853–872.

Van Landeghem, K.J.J., Uehara, K., Wheeler, A.J., Mitchell, N.C. & Scourse, J.D. (2009) Post-glacial sediment dynamics in the Irish Sea and sediment wave morphology: data–model comparisons. *Continental Shelf Research*, 29, 1723–1736.

Lee, K.C., Webster, J.M., Salles, T., Mawson, E.E. & Hill, J. (2022) Tidal dynamics drive ooid formation in the Capricorn Channel since the Last Glacial Maximum. *Marine Geology*, 454, 106944.

Lewis, M., Neill, S., Robins, P. & Hashemi, M. (2015) Resource assessment for future generations of tidal-stream energy arrays. *Energy*, 83, 403–415.

Van der Molen, J. & De Swart, H.E. (2001) Holocene tidal conditions and tide-induced sand transport in the southern North Sea. *Journal of Geophysical Research: Oceans*, 106, 9339–9362.

Mortimer, T.A.L., Scourse, J.D., Ward, S.L. & Uehara, K. (2013) Simulated late-glacial and Holocene relative sea-level and palaeo-tidal changes on the Isles of Scilly: a new approach for assessing changes in the areal extent of the inter-tidal zone. *Geoscience in South-West England*, 13, 152–158.

Neill, S.P., Scourse, J.D. & Uehara, K. (2010) Evolution of bed shear stress distribution over the northwest European shelf seas during the last 12,000 years. *Ocean Dynamics*, 60, 1139–1156.

Peltier, W.R. (1994) Ice-age palaeotopography. *Science*, 265, 195–201.

R Core Team. (2023) R: a language and environment for statistical computing. R Foundation for Statistical Computing, Vienna, Austria. URL https://www.R-project.org/

Richardson, N., Cook, I., Crane, N. et al. (2023) Arrow: Integration to 'Apache' 'Arrow'. https://arrow.apache.org/docs/r/; https://github.com/apache/arrow/

Rippeth, T.P., Scourse, J.D., Uehara, K. & McKeown, S. (2008) Impact of sea-level rise over the last deglacial transition on the strength of the continental shelf CO_2 pump. *Geophysical Research Letters*, 35, L24604.

Robins, P.E., Neill, S.P., Lewis, M.J. & Ward, S.L. (2015) Characterising the spatial and temporal variability of the tidal-stream energy resource over the northwest European shelf seas. *Applied Energy*, 147, 510–522.

Schmittner, A., Green, J.A.M. & Wilmes, S.B. (2015) Glacial ocean overturning intensified by tidal mixing in a global circulation model. *Geophysical Research Letters*, 42, 4014–4022.

Scourse, J.D. (2013) Quaternary sea-level and palaeotidal changes: a review of impacts on, and responses of, the marine biosphere. *Oceanography and Marine Biology: An Annual Review*, 51, 1–70.

Scourse, J.D., Austin, W.E.N., Long, B.T., Assinder, D.J. & Huws, D. (2002) Holocene evolution of seasonal stratification in the Celtic Sea: refined age model, mixing depths and foraminiferal stratigraphy. *Marine Geology*, 191, 119–145.

Scourse, J., Uehara, K. & Wainwright, A. (2009) Celtic Sea linear tidal sand ridges, the Irish Sea Ice Stream and the Fleuve Manche: palaeotidal modelling of a transitional passive margin depositional system. *Marine Geology*, 259, 102–111.

Shchepetkin, A.F. & McWilliams, J.C. (2005) The regional oceanic modeling system (ROMS): a split-explicit, free-surface, topography-following-coordinate oceanic model. *Ocean Modelling*, 9, 347–404.

Shennan, I., Bradley, S., Milne, G., Brooks, A., Bassett, S. & Hamilton, S. (2006) Relative sea-level changes, glacial isostatic modelling and ice-sheet reconstructions from the British Isles since the Last Glacial Maximum. *Journal of Quaternary Science*, 21, 585–599.

Shennan, I., Lambeck, K., Flather, R., Horton, B., McArthur, J., Innes, J. et al. (2000) Modelling western North Sea palaeogeographies and tidal changes during the Holocene. *Special Publication of the Geological Society*, 166, 299–319.

Sievert, C., Cheng, J. & Aden-Buie, G. (2023) bslib: custom 'Bootstrap' 'Sass' themes for 'shiny' and 'rmarkdown'. https://rstudio.github.io/bslib/.; https://github.com/rstudio/bslib

Simpson, J.H. & Hunter, J.R. (1974) Fronts in the Irish sea. *Nature*, 250(5465), 404–406.

Sulzbach, R., Klemann, V., Knorr, G., Dobslaw, H., Dümpelmann, H., Lohmann, G. et al. (2023) Evolution of global ocean tide levels since the Last Glacial Maximum. *Paleoceanography and Paleoclimatology*, 38, e2022PA004556.

Uehara, K., Saito, Y. & Hori, K. (2002) Paleotidal regime in the Changjiang (Yangtze) Estuary, the East China Sea, and the Yellow Sea at 6 ka and 10 ka estimated from a numerical model. *Marine Geology*, 183, 179–192.

Uehara, K., Scourse, J.D., Horsburgh, K.J., Lambeck, K. & Purcell, A.P. (2006) Tidal evolution of the northwest European shelf seas from the Last Glacial Maximum to the present. *Journal of Geophysical Research: Oceans*, 111, C09025.

Vasskog, K., Svendsen, J.I., Mangerud, J., Haaga, K.A., Svean, A. & Lunnan, E.M. (2019) Evidence of early deglaciation (18 000 cal a BP) and a postglacial relative sea-level curve from southern Karmøy, south-west Norway. *Journal of Quaternary Science*, 34, 410–423.

Wang, S., Ge, J., Kilbourne, K.H. & Wang, Z. (2020) Numerical simulation of mid-Holocene tidal regime and storm-tide inundation in the south Yangtze coastal plain, East China. *Marine Geology*, 423, 106134.

Ward, S.L., Neill, S.P., Scourse, J.D., Bradley, S.L. & Uehara, K. (2016) Sensitivity of palaeotidal models of the northwest European shelf seas to glacial isostatic adjustment since the Last Glacial Maximum. *Quaternary Science Reviews*, 151, 198–211.

Ward, S.L., Scourse, J.D., Yokoyama, Y. & Neill, S.P. (2020) The challenges of constraining shelf sea tidal models using seabed sediment grain size as a proxy for tidal currents. *Continental Shelf Research*, 205, 104165.

Wessel, P. & Smith, W.H.F. (1996) A global, self-consistent, hierarchical, high-resolution shoreline database. *Journal of Geophysical Research: Solid Earth*, 101, 8741–8743.

Wickham, H., Averick, M., Bryan, J., Chang, W., McGowan, L., François, R. et al. (2019) Welcome to the tidyverse. *Journal of Open Source Software*, 4, 1686. Available at https://doi.org/10.21105/joss.01686

Wilmes, S.B. & Green, J.A.M. (2014) The evolution of tides and tidal dissipation over the past 21,000 years. *Journal of Geophysical Research: Oceans*, 119, 4083–4100.

Wilmes, S.B., Green, J.M. & Schmittner, A. (2021) Enhanced vertical mixing in the glacial ocean inferred from sedimentary carbon isotopes. *Communications Earth & Environment*, 2, 166.

Woods, M.A., Wilkinson, I.P., Leng, M.J., Riding, J.B. Vane, C.H., dos Santos, R.A.L. et al. (2019) Tracking Holocene palaeostratification and productivity changes in the western Irish Sea: a multi-proxy record. *Palaeogeography, Palaeoclimatology, Palaeoecology*, 532, 109–231.